University of Birmingham

Gold-Induced Desulfurization in a Bis(ferrocenyl) Alkane Dithiol

Pensa, Evangelina; Karpowicz, Rafa; Jaboski, Artur; Trzybiski, Damian; Woniak, Krzysztof; Šaki, Davor; Vrek, Valerije; Long, Nicholas J.; Albrecht, Tim; Kowalski, Konrad

[Link to publication on Research at Birmingham portal](#)

Gold-induced desulfurisation in a bis(ferrocenyl) alkane dithiol

Evangelina Pensa,[a] Rafał Karpowicz,[b] Artur Jabłoński,[b] Damian Trzybiński,[c] Krzysztof Woźniak,[c] Davor Šakić,[d] Valerije Vrček,[d] Nicholas J. Long,[a] Tim Albrecht,* [a,e] and Konrad Kowalski*[b]

[a] Department of Chemistry, Imperial College London, Molecular Sciences Research Hub, London, W12 0BZ, UK

[b] Faculty of Chemistry, Department of Organic Chemistry, University of Łódź, Tamka 12, 91-403 Łódź, Poland

[c] Faculty of Chemistry, Biological and Chemical Research Centre, University of Warsaw, Żwirki i Wigury 101, 02-089 Warszawa, Poland

[d] Faculty of Pharmacy and Biochemistry, University of Zagreb, Ante Kovačića 1, 10000 Zagreb, Croatia

[e] School of Chemistry, University of Birmingham, Edgbaston, Birmingham, B15 2TT, UK

TOC
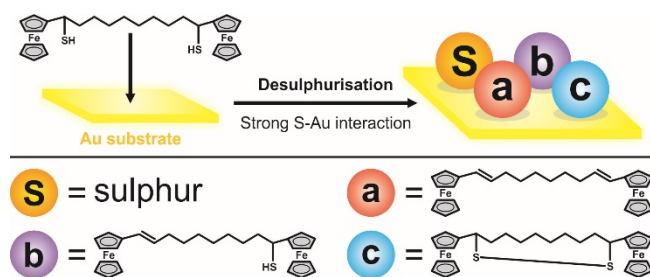
Abstract

Thiol-modified ferrocenes on gold have been archetypical model systems for many fundamental charge transfer and other studies, since both thiol-gold and ferrocene redox chemistry are considered to be well-understood. Thus unexpectedly, we found that for a representative of a new class of flexibly linked bis-ferrocenyl compounds, namely 1-10-bis(1-ferrocenyl)decane dithiol, surface immobilization on gold failed. Instead, in the presence of gold, molecular decomposition took place, resulting in sulfur-based adlayers and well-defined molecular elimination products, for which we provide spectroscopic evidence. Careful control experiments and comparison with related ferrocene compounds provide insight into the mechanism of the observed elimination reactions, as a combined effect of the molecular structure and the nature of the gold/sulfur bond. These findings, thus, have broader impact on the design of molecular adlayers, for example, in the context of surface functionalisation in sensing or the synthesis of gold nanoparticles.

INTRODUCTION

Ferrocene (FcH) is an iconic organometallic molecule featuring a characteristic sandwich-like molecular structure, significant thermal stability and inertness towards air and moisture.[1-6] Ferrocenyl (Fc) derivatives have found numerous applications across chemistry, biology and material sciences.[7-17] An important property of FcH is that it undergoes a one-electron oxidation which is reversible and produces the ferrocenium cation ($FeCp_2^+$) as a (relatively) stable product. This electrochemical behavior is inherited by many FcH derivatives and contributes to their usefulness towards various applications. Representative examples of such applications comprise utilization of Fc-based ligands in the design of redox-switched catalysis for lactide polymerization[18] and utilization of Fc groups as redox-activating antenna in ferrocifen-type anticancer agents.[17] Moreover, FcH-containing compounds have been well-studied in the context of molecular electronics, redox-active self-assembled monolayers

(SAM), mixed valent (MV) systems and nonlinear optical materials (NLO).[19-41] Surface immobilization on gold and some related metals is often achieved *via* thiol, thioether and other sulfur-containing functionalities as the anchor group[42-44] with either 1- or 1,1'-disubstituted ferrocenes as well-established model systems.

We have a long standing interest in redox-active molecular electronic components in the context of single-molecule charge transport studies,[45] including single-center Os- and Co-based systems,[46-49] small nanoparticles,[50] viologens,[51] in ex situ and in electrolytes and in ionic liquids.[52] In this context, charge transport in the hopping regime, i.e. directly involving the redox centres in the transport pathway, has been relatively well studied, highlighting the link between tunnelling conductance and the hopping constants.[49,53,54] On the other hand, branched and ring-shaped redox-active systems, or systems where redox-active pendant groups affect the charge transport pathway indirectly are less well-studied,[20,22-25,37-39] even though they can display interesting quantum interference features such as Breit-Wigner and Fano resonances.[55] Some of the systems studied here could offer interesting insight, so we herein report the synthesis, structural and electrochemical characterization of representatives of a new class of flexibly linked bis-Fcs. We have focused on 1,10-bis(1-ferrocenyl)decane-1,10-dithiol **3** (Scheme 1) with thiol anchor groups intended for surface immobilisation on electrode substrates, such as gold. Interestingly, however, **3** did not interact with the gold substrate in the expected way, *viz* forming a stable gold-sulfur bond. While the characteristic voltammetric FcH-based redox signal was present after incubation of the gold substrate, increased with immersion time and displayed the electrochemical characteristics of an immobilised redox species, comprehensive characterisation of the substrate by surface voltammetry, Scanning Tunnelling Microscopy (STM) imaging and X-ray Photoelectron Spectroscopy (XPS) revealed a more complex picture. Specifically, it was found that an adlayer of elemental sulfur was present on the substrate with an associated reductive

desorption charge about an order of magnitude larger than the charge associated with the FcH redox process. According to the molecular design, the ratio between Fc and thiol groups was expected to be unity, which was indeed confirmed by elemental analysis. Analysis of the solution composition by plate chromatography/electron spray ionisation mass spectrometry (EI-MS) further showed the presence of unsaturated, (partly) de-thiolated derivatives of **3**, which were not formed in the absence of Au or with non-thiol containing analogs of **3**. Thus, the presence of both gold and the thiol functionality were required to trigger the observed reaction. Notably, such instabilities have not been reported for FcHs featuring even very short primary alkane thiols as substituents.[26,27] Thus, it seems that in addition to the above conditions, the close proximity of the Fc and the thiol group, as well as the secondary nature of the thiol are pre-requisites for the process to take place. Finally, we note that immobilisation of **3** continues to take place even after the sulfur layer has formed. This would imply that this layer is either sufficiently porous that **3** continues to have access to the gold surface or, more likely, that **3** binds to the sulfur layer itself.

RESULTS AND DISCUSSION

The preparation of 1,10-bis(1-ferrocenyl)decane-1,10-dithiol **3** involves three steps and is depicted in Scheme 1.
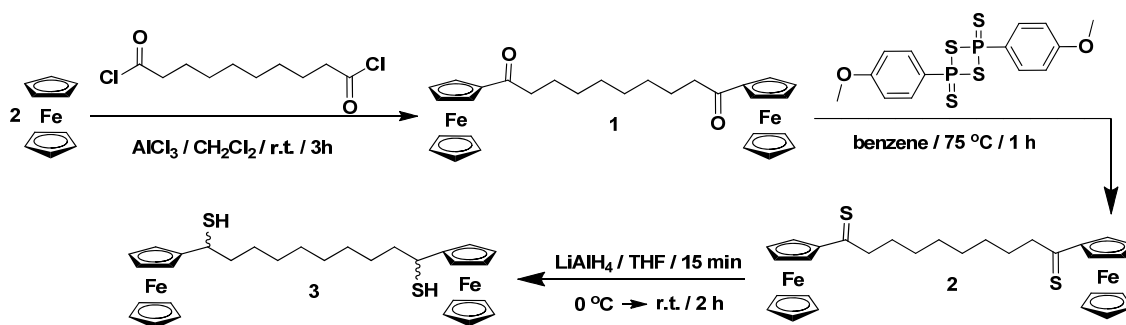
Scheme 1. Synthesis of compounds **1-3**

In the first step, the 1,10-bis(1-ferrocenyl)decane-1,10-dione **1** was prepared in a Friedel-Crafts reaction of FcH with sebacoyl chloride in the presence of AlCl$_3$ (orange crystalline solid, 87% yield; see SI for further characterisation). Ferrocenyl diketone **1** has been reported in 1986 as a side product of some acylation reactions of FcH.[56] More recently, Bulut and co-workers obtained **1** in 90% yield in a Friedel-Crafts reaction of FcH with sebacoyl chloride in the presence of EtAlCl$_2$.[57] These authors concluded that the high yield of the reaction results from EtAlCl$_2$ being applied as a catalyst. Our results, however, importantly show that using a common AlCl$_3$ catalyst also allows the isolation of **1** in high yield.

In the second step, compound **1** was treated with Lawesson's reagent to afford the 1,10-bis(1-ferrocenyl)decane-1,10-dithione **2** as a dark blue oil in 72% yield. Dithioketone **2** is an unstable compound which undergoes rapid decomposition to produce a mixture of ill-defined products. Despite its unstable nature, we were able to confirm the presence of **2** by ^{1}H NMR and IR spectroscopy as well as by mass spectrometry, see SI. In the third step, the thioketone functions in **2** were reduced with LiAlH$_4$ in tetrahydrofuran at 0°C to produce the 1,10-bis(1-ferrocenyl)decane-1,10-dithiol **3** (yellow oil, 73% yield, see SI for further characterisation).

The redox behavior of compounds **1** and **3** in solution, as studied by cyclic voltammetry (CV) and differential pulse voltammetry (DPV) with a glassy carbon as working electrode, features a single pair of redox peaks, associated with the oxidation/reduction of the Fc units (see panel ii) in Figures S1 a/b).[58,59] The process appears to involve a reversible single-electron transition as: (1) the peak-to-peak separation (ΔE$_p$) is close to the predicted value of 59 mV, and (2) current density ratio (j$_{pa}$/j$_{pc}$) ≈ 1, Figure S1 a/b panels iii) and iv). We did not observe any evidence for peak splitting from the two FcH centres in CV or DPV, suggesting that there is no significant electronic interaction between them. We attribute this to

the relatively large Fc–Fc distance (15.718 Å, Fe/Fe)[60] and the aliphatic nature of the linker as well as efficient screening by the supporting electrolyte, as has been observed for analogous systems.[61-63] Taken together, these data suggest that both **1** and **3** undergo two simultaneous single-electron transitions involving the two Fc centres in each molecule, rather than a single two-electron process. During these experiments, we did not observe any changes in the electrochemical response that would suggest molecular decomposition (see consecutive cycles in panel ii) of Figures S1 a/b).

After electrochemical characterization in solution, we proceeded to investigate the properties of immobilised **3**, *viz* bound to Au substrates via the thiol functionalities. To this end, both the redox response of the Fc centres and the reduction of the Au/S bond can, in principle, be used to monitor the adsorption of **3** over time, as the associated charges are proportional to the surface coverage.
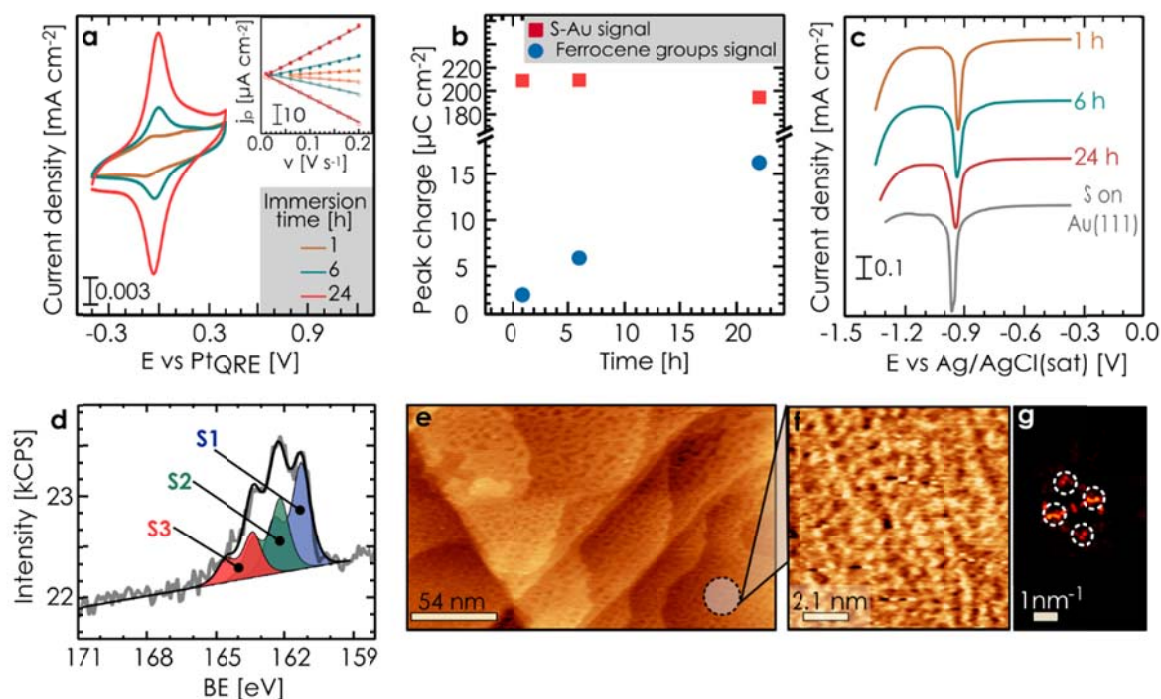

Figure 1. a) CVs of **3** showing the redox signal from the Fc centres, as a function of the immersion time (Au(111) substrate, scan rate v = 0.1 V/s, electrolyte: 0.1 M TBA PF$_6$ in DCM). Inset: Peak current density vs. v. b) Integrated peak charge from a) (blue circles) and

the reductive desorption data shown in c) (red squares). c) Reductive desorption of S-Au bonds, as a function of immersion time (v = 0.1 V/s, electrolyte: 0.1 M NaOH). d) XP spectra of the S2p signal (grey curve) showing three different S environments, namely S1, S2 and S3. e) STM image of the Au(111) surface after incubation with **3**, showing typical pit formation (dark areas). f) Magnified area from e), revealing a quasi-rectangular pattern with characteristic distances of 1.0 ± 0.1 nm and 0.92 ± 0.089 nm. g) Fast Fourier Transform (FFT) of f).

In accordance with these expectations, we indeed observed a notable increase in the Fc redox signal as a function of immersion time, as shown in Figure 1a. The peak separation ΔE_p was small with 26 ± 7 mV, albeit not zero, presumably as a result of the changing microenvironment of the redox centers.[27] The anodic and cathodic peak currents increase linearly with v (inset). Notably, even after 24 h immersion time, the peak charge and hence the surface coverage still do not seem to have become saturated (16 μC·cm^{-2} after 24 h, as shown in panel b), which is unusually slow for the adsorption of small thiols onto Au.[64]

For comparison, panel c) shows the reductive desorption data, for different immersion times in dichloromethane solutions of **3** and recorded in 0.1 M NaOH electrolyte (pH = 13), see Methods for further details. All curves display a sharp, cathodic peak centered at -0.93 ± 0.02 V that is characteristic of S-Au bond reduction.[65]

However, compared to the Fc-based redox response, a very different picture emerges. Firstly, the peak charge does not change significantly for immersion times between 1 and 24 h, with an average peak charge of 204 ± 18 μC·cm^{-2} (panel c). Secondly, the associated charge is more than an order of magnitude larger than the value determined from the Fc response, which cannot be accounted for by differences in the electron transfer stoichiometry. Equally, sulfur-based contaminants in the chemicals and solvents used could be ruled out as the source of the sulfur species, because in control experiments in the absence of **3** no adsorbed sulfur could be detected, while elemental analysis of **3** did not show any excess sulfur species in the

solid. Desulfurisation of **3** was thus the most likely origin of the sulfur adlayer, which was supported by reductive desorption experiments with sulfide-modified Au(111), Figure 1c (grey curve). Namely, after immersing the substrate in 0.1 M aqueous Na_2S (pH = 13) for 5 minutes, the reductive desorption curve was characterized by a sharp cathodic peak centred at ca. -0.9 V with a charge density of 192 $\mu C \cdot cm^{-2}$ (S-Au + 2e$^-$ → 2Au + S^{2-}), a value comparable to the one found after incubation with **3**, *vide supra*. It is worth noting that the FcH signal kept increasing, even after the sulfur adlayer had already formed, suggesting immobilisation of **3** directly on sulfur rather than Au.

X-ray photoelectron spectroscopy (XPS) characterisation of the surface after 1 h incubation with **3** confirmed the presence of a sulfur-rich layer and provided further insight into its speciation, Figure 1d (S2p region). The signal was successfully fitted with 3 components namely S1, S2 and S3 (each a characteristic doublet with relative intensities of 1:2 associated with quantum numbers j = 1/2 and 3/2). The extracted binding energies of S $2p_{3/2}$ were centered at 161.3 eV for S1, 162.2 eV for S2 and 163.4 eV for S3 with an intensity ratio of 2.3:1.6:1. As reported previously,[66] the more intense signal S1 was assigned to the presence of a sulfide adlayer, while S2 and S3 have been associated with either polysulfide or thiolate (S2), and elemental sulfur or physisorbed thiols (S3), respectively.

Desulfurisation of thiols in contact with Au substrates has been observed previously, in particular for aromatic thiols and those with good leaving groups (i.e. where the decomposition product is relatively stable).[67-70] However, while their results confirmed the formation of a sulfur-rich layer on the substrate from a range of different organic thiols, no direct experimental evidence for the reaction products in solution were reported. This would nevertheless be useful, in order to gain further insight into the reaction mechanism and to assess potential further implications of the effect.

Since here, the amount of molecular by-products is expected to scale with the available Au surface area, we decided to replace the macroscopic Au(111) substrate with a dispersion of citrate-stabilised Au colloids (diameter: 10 nm) and to analyse the solution composition using plate chromatography/electron impact mass spectrometry (EI-MS).

After incubation of **3** in the colloidal dispersion (in THF, particle concentration: $4 \cdot 10^{12}$ particles/mL) for 24 hours in the dark, three different molecular species could be detected, namely the de-thiolated product **4**, the oxidized di-sulfide **5** and the partially de-thiolated product **6**, Figure 2. As a control, the same experiment was performed in the absence of nanoparticles, but no decomposition products were detected.

With the aim to fully characterize the decomposition products, their isolation on a preparative scale was attempted. Unfortunately, all attempts were unsuccessful. However, we did successfully synthesise the proposed compound **4** (Figure S7), which is likely to be the abundant decomposition product according to the relative intensity of the EI-MS (Figures S8-S10). The EI-MS spectrum of synthetized compound **4** shows the M+ peak at 506 m/z (Figure S11), confirming its presence as one of the decomposition products. Furthermore, as the same peak at 506 m/z is present in the EI-MS spectra of all decomposition fractions (Figures S8-S10), it can be hypothesised that compound **4** is the most stable reaction product and compounds **5** and **6** decompose either in the course of MS measurement or in the bulk to end up with the most stable alkene **4**. In fact, in control experiments with compound **4** in contact with colloidal gold, no decomposition of **4** was found reinforcing all above mentioned. The position of the double bonds in the chain of **4** has been assigned based on ^{1}H-NMR spectrum. ^{1}H-NMR of compound **4** shows the unambiguously characteristic doublet and doublet of triplet signals assigned to the two CH=CH bonds (Figure S7). This signal pattern can only result from terminal positioning of the C=C bonds in the chain as another position of the C=C bond would lead to more complex features in the spectrum.
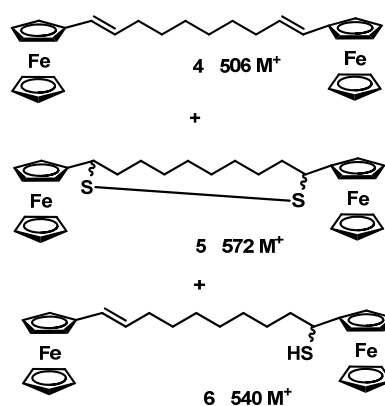
Figure 2. Reaction products **4**, **5**, and **6** (inc. M$^+$ ion masses of 506, 572 and 540), detected after incubation of **3** with Au nanoparticle dispersion.

Hence, these results confirm the formation of well-defined molecular reaction products that are complementary to the formation of the sulfur adlayer. It is interesting to note that such a decomposition process has not been observed with the unsubstituted FeCp analogues of 2-alkyl mercaptans[71] or other thiol-modified FcHs, even when the thiol group was very close to the Cp ring. [26,27] The latter is, therefore, not a sufficient pre-requisite for the reaction to take place under the conditions used here. Arguably, those molecules feature primary thiol groups, rather than secondary ones as in **3**, and the position of the Fc group, relative to the thiol, in the former case does not lend itself to the stabilisation of potential intermediates in the same way. It is therefore likely that both play a role in the de-sulfurisation of **3**, namely the ability to form C/C double bonds in β-position and the stabilisation effect of the Fc group in proximity.

CONCLUSIONS

We report a new three-step approach for the synthesis for flexibly linked bis(1-Fc) compounds in high yield and, in contrast to previous studies, have utilised AlCl$_3$ as the catalyst. This further expands the toolset available for the design of FcH-based materials.

Secondly, failed attempts to immobilise the thiol-modified variant **3** on gold by exploiting well-known gold/thiol chemistry highlights some of the complexities in this interaction. Facilitated by the strong gold/thiol interaction, desulfurisation occurs producing sulfur-containing adlayers on the gold substrate and well-defined, unsaturated molecular products in solution. Unexpectedly, some surface immobilisation of **3** took place even after the sulfur layer had formed. Based on electrochemical, XPS, STM, chromatography/EI-MS, we provide comprehensive characterisation and speciation evidence of both the surface layer and the molecular products, offering valuable insight into the mechanism of decomposition and hence into the rules underpinning the design of well-defined molecular adlayers. Such considerations most likely go beyond the specific system under study here and extend towards other areas where thiol-based self-assembled monolayers are key, e.g. in sensor design and nanoparticle stabilisation.

ASSOCIATED CONTENT

Supporting Information. The Supporting information is available free of charge via the Internet at http://pubs.acs.org.

Synthetic procedures for **1-3**; reaction of **3** with Au nanoparticles; cyclic voltammetry and differential pulse voltammetry data for **1** and **3**; ^{1}H NMR spectra of **1**, **2**, **3** and 4 in $CDCl_3$; ^{13}C NMR spectra of **1** and **3** in $CDCl_3$; mass spectrometry of **4**, **5** and **6**; XRD data for **1**; X-ray photoelectron spectroscopy of **3** on Au substrate. DFT structure optimization details.

AUTHOR INFORMATION

Corresponding Authors

* t.albrecht@bham.ac.uk and konrad.kowalski@chemia.uni.lodz.pl

Notes

The authors declare no competing financial interests.

ACKNOWLEDGMENTS

REFERENCES

(1) Kealy, T. J.; Pauson, P. L. A New Type of Organo-Iron Compound. *Nature* **1951**, *168*, 1039-1040.

(2) Miller, S. A.; Tebboth, J. A.; Tremaine, J. F. Dicyclopentadienyliron. *J. Chem. Soc.* **1952**, 632-635.

(3) Wilkinson, G.; Rosenblum, M.; Whiting, M. C.; Woodward, R. B. The Structure of Iron Bis-cyclopentadienyl. *J. Am. Chem. Soc.* **1952**, *74*, 2125-2126.

(4) Woodward, R. B.; Rosenblum, M.; Whiting, M. C. A New Aromatic System. *J. Am. Chem. Soc.* **1952**, *74*, 3458-3459.

(5) Fisher, E. O.; Pfab, W. Cyclopentadien-Metallkomplexe, ein neuer Typ metallorganischer Verbindungen. *Z. Naturforsch.* **1952**, *76*, 377-379.

(6) Dunitz, J. D.; Orgel, L. E. Bis-cyclopentadienyl Iron: a Molecular Sandwich. *Nature* **1953**, *171*, 121-122.

(7) Togni, A.; Hayashi, T (Eds.), Ferrocenes: Homogeneous Catalysis, Organic Synthesis, Material Science, Wiley-VCH, Weinheim, **1995**.

(8) Štěpnička, P. (Ed.), Ferrocenes: Ligands, Materials and Biomolecules, Wiley-VCH, Chichester, **2008**.

(9) Dai, L.-X.; Hou, X.-L. (Eds.), Chiral Ferrocenes in Asymmetric Catalysis, Wiley-VCH, Weinheim, **2010**.

(10) Manners, I. (Ed.), Synthetic Metal-Containing Polymers, Wiley-VCH, Weinheim, 2004.

(11) Long, N.J. Metallocenes-An Introduction to Sandwich Complexes, Blackwell Science, Oxford, **1998**.

(12) Štěpnička, P. (Ed.), Special Issue: The Multifaced Chemistry of Ferrocene, *Eur. J. Inorg. Chem.* **2017**, 212-526.

(13) K. Heinze, K.; Lang H. (Eds.), Special Issue: Ferrocene-Beauty and Function, *Organometallics* **2013**, *32*, 5623-6146.

(14) van Stavern, D. R.; Metzler-Nolte, N. Bioorganometallic Chemistry of Ferrocene. *Chem. Rev.* **2004**, *104,* 5931-5985.

(15) Ornelas, C. Application of ferrocene and its derivatives in cancer research. *New J. Chem.* **2011**, *35*, 1973-1985.

(16) Kowalski, K. Ferrocenyl-nucleobase complexes: Synthesis, chemistry and applications. *Coord. Chem. Rev.* **2016**, *317*, 132-156

(17) Jaouen, G.; Vessières, A.; Top, S. Ferrocifen type anti cancer drugs. *Chem. Soc. Rev.* **2015**, *44*, 8802-8817.

(18) Gregson, C.K.A.; Gibson, V.C.; Long, N.J.; Marshall, E.L.; Oxford, P.J.; White, A.J.P. Redox Control within Single-Site Polymerization Catalysts. *J. Am. Chem. Soc.* **2006**, *128*, 7410–7411.

(19) Carroll, R. L.; Gorman, C. B. The Genesis of Molecular Electronics. *Angew. Chem. Int. Ed.* **2002**, *41*, 4378-4400.

(20) Inkpen, M. S.; White, A. J. P.; Albrecht, T.; Long, N. J. Avoiding problem reactions at the ferrocenyl-alkyne motif: a convenient synthesis of model, redox-active complexes for molecular electronics. *Dalton Trans*. **2014**, *43*, 15287-15290.

(21) Diallo, A. K.; Absalon, C.; Ruiz, J.; Astruc, D. Ferrocenyl-Terminated Redox Stars: Synthesis and Electrostatic Effects in Mixed-Valence Stabilization. *J. Am. Chem. Soc.* **2011**, *133*, 629-641.

(22) Inkpen, M. S.; Scheerer, S.; Linseis, M.; White, A. J. P.; Winter, R. F.; Albrecht, T.; Long, N. J. Oligomeric ferrocene rings. *Nat. Chem*. **2016**, *8*, 825-830.

(23) Wilson, L. E.; Hassenrück, C.; Winter, R. F.; White, A. J. P.; Albrecht, T.; Long, N. J. Ferrocene- and Biferrocene-Containing Macrocycles towards Single-Molecule Electronics. *Angew. Chem. Int. Ed.* **2017**, *56*, 6838-6842.

(24) Wilson, L. E.; Hassenrück, C.; Winter, R. F.; White, A. J. P.; Albrecht, T.; Long, N. J. Functionalised Biferrocene Systems towards Molecular Electronics. *Eur. J. Inorg. Chem.* **2017**, 496-504.

(25) Inkpen, M. S.; Albrecht, T.; Long N. J. Branched Redox-Active Complexes for the Study of Novel Charge Transport Processes. *Organometallics* **2013**, *32*, 6053-6060.

(26) Nerngchamnong, N.; Wu, H.; Sotthewes, K.; Yuan, L.; Cao, L.; Roemer, M.; Lu, J.; Loh, K. P.; Troadec, C.; Zandvliet, H. J. W.; Nijhuis, C. A. Supramolecular Structure of Self-Assembled Monolayers of Ferrocenyl Terminated *n*-Alkanethiolates on Gold Surfaces. *Langmuir* **2014**, *30*, 13447-13455.

(27) Nerngchamnong, N.; Wu, H.; Sotthewes, K.; Yuan, L.; Cao, L.; Roemer, M.; Lu, J.; Loh, K.P.; Troadec, C.; Zandvliet, H.J.W.; Nijhuis, C.A. Nonideal Electrochemical Behavior of Ferrocenyl–Alkanethiolate SAMs Maps the Microenvironment of the Redox Unit. *J. Phys. Chem. C* **2015**, *119*, 21978-21991.

(28) Bertin, P. A.; Georganopoulou, D.; Liang, T.; Eckermann, A. L.; Wunder, M.; Ahrens, M. J.; Blackburn, G. F.; Meade, T. J. Electroactive Self-Assembled Monolayers on Gold via Bipodal Dithiazepane Anchoring Groups. *Langmuir* **2008**, *24*, 9096-9101.

(29) Kitagawa, T.; Matsubara, H.; Komatsu, K.; Hirai, K.; Okazaki, T.; Hase, T. Ideal Redox Behavior of the High-Density Self-Assembled Monolayer of a Molecular Tripod on a Au(111) Surface with a Terminal Ferrocene Group. *Langmuir* **2013**, *29*, 4275-4282.

(30) Breuer, R.; Schmittel, M. Redox-Stable SAMs in Water (pH 0–12) from 1,1′-Biferrocenylene-Terminated Thiols on Gold. *Organometallics* **2012**, *31*, 6642-6651.

(31) Shaporenko, A.; Rössler, K.; Lang, H.; Zharnikov, M. Self-Assembled Monolayers of Ferrocene-Substituted Biphenyl Ethynyl Thiols on Gold. *J. Phys. Chem. B* **2006**, *110*, 24621-24628.

(32) Chen, C-P.; Luo, W-R.; Chen, C-N.; Wu, S-M.; Hsieh, S.; Chiang, C-M.; Dong, T-Y. Redox-Active π-Conjugated Organometallic Monolayers: Pronounced Coulomb Blockade Characteristic at Room Temperature. *Langmuir* **2013**, *29*, 3106-3115.

(33) Umeda, K.; Fukui, K. Observation of Redox-State-Dependent Reversible Local Structural Change of Ferrocenyl-Terminated Molecular Island by Electrochemical Frequency Modulation AFM. *Langmuir* **2010**, *26*, 9104-9110.

(34) Frasconi, M.; D'Annibale, A.; Favero, G.; Mazzei, F.; Santucci, R.; Ferri, T. Ferrocenyl Alkanethiols−Thio β-Cyclodextrin Mixed Self-Assembled Monolayers: Evidence of Ferrocene Electron Shuttling Through the β-Cyclodextrin Cavity. *Langmuir* **2009**, *25*, 12937-12944.

(35) Pfaff, U.; Filipczyk, G.; Hildebrandt, A.; Korb, M.; Lang, H. 1,3,5-Triferrocenyl-2,4,6-tris(ethynylferrocenyl)-benzene – a new member of the family of multiferrocenyl-functionalized cyclic systems. *Dalton. Trans*. **2014**, *43*, 16310-16321.

(36) Speck, J. M.; Korb, M.; Rüffer, T.; Hildebrandt, A.; Lang, H. Substituent Influence on Charge Transfer Interactions in α,α′-Diferrocenylthiophenes. *Organometallics* **2014**, *33*, 4813-4823.

(37) Kowalski, K.; Karpowicz, R.; Mlostoń, G.; Miesel, D.; Hildebrandt, A.; Lang, H.; Czerwieniec, R.; Therrien, B. Synthesis and (spectro)electrochemistry of mixed-valent diferrocenyl–dihydrothiopyran derivatives. *Dalton. Trans*. **2015**, *44*, 6268-6276.

(38) Kowalski, K.; Szczupak, Ł.; Skiba, J.; Abdel-Rahman, O. S.; Winter, R. F.; Czerwieniec, R.; Therrien, B. Synthesis, Structure, and Spectroelectrochemistry of Ferrocenyl–Meldrum's Acid Donor–Acceptor Systems. *Organometallics* **2014**, *33*, 4697-4705.

(39) Kowalski, K.; Linseis, M.; Winter, R. F.; Zabel, M.; Záliš, S.; Kelm, H.; Krüger, H.-J.; Sarkar, B.; Kaim, W. Charge Delocalization in a Heterobimetallic Ferrocene−(Vinyl)Ru(CO)Cl(P^{i}Pr$_3$)$_2$ System. *Organometallics* **2009**, *28*, 4196-4209.

(40) Heck, J.; Dabek, S.; Meyer-Friedrichsen, T.; Wong, H. Mono- and dinuclear sesquifulvalene complexes, organometallic materials with large nonlinear optical properties. *Coord. Chem. Rev*. **1999**, *190-192*, 1217-1254.

(41) Aguirre-Etcheverry, P.; O'Hare, D. Electronic Communication through Unsaturated Hydrocarbon Bridges in Homobimetallic Organometallic Complexes. *Chem. Rev.* **2010**, *110*, 4839-4864.

(42) Reed, M. A.; Zhou, C.; Muller, C. J.; Burgin, T. P.; Tour, J. M. Conductance of a Molecular Junction. *Science* **1997**, *278*, 252-254.

(43) Lavrich, D. J.; Wetterer, S. M.; Bernasek, S. L.; Scoles, G. Physisorption and Chemisorption of Alkanethiols and Alkyl Sulfides on Au(111). *J. Phys. Chem. B* **1998**, *102*, 3456-3465.

(44) Leavy, M. C.; Bhattacharyya, S.; Cleland, W. E.; Hussey, C. L. Electrochemical and Spectroscopic Characterization of Self-Assembled Monolayers of Unsymmetrical Ferrocenyl Dialkyl Sulfide Derivatives on Gold. *Langmuir* **1999**, *15*, 6582-6586.

(45) Zhang, J.; Kuznetsov, A. M.; Medvedev, I. G.;Chi, Q.; Albrecht, T.; Jensen, P. S.; Ulstrup, J. Single-molecule Electron Transfer in Electrochemical Environments. *Chem. Rev.* **2008**, *108*, 2737-2791.

(46) Albrecht, T.; Guckian, A.; Ulstrup, J.; Vos, J. G. Transistor Effects and in situ STM of Redox Molecules at Room Temperature, *IEEE Trans. Nanotech.* **2005**, *4*, 430-434.

(47) Albrecht, T.; Guckian, A.; Ulstrup, J.; Vos, J. G. Transistor-like Behavior of Transition Metal Complexes, *Nano Lett.* **2005**, *5*, 1451-1455.

(48) Albrecht, T.; Moth-Poulsen, K.; Christensen, J. B.; Guckian, A.; Bjørnholm, Th.; Vos, J. G.; Ulstrup, J. In situ scanning tunnelling spectroscopy of inorganic transition metal complexes, *Faraday Discuss.* **2006**, *131*, 265-279.

(49) Albrecht, T.; Guckian, A.; Kuznetsov, A. M.; Vos, J. G.; Ulstrup, J. Mechanism of electro-chemical charge transport in individual transition metal complexes, *J. Am. Chem. Soc.*, **2006**, *128*, 17132 – 17133.

(50) Albrecht, T.; Mertens, S. F. L.; Ulstrup, J. Intrinsic Multi-state Switching of Gold Clusters through Electrochemical Gating, *J. Am. Chem. Soc.* **2007**, *129*, 9162-9167.

(51) Haiss, W.; Albrecht, T.; van Zalinge, H.; Higgins, S. J.; Bethell, D.; Höbenreich, H.; Schiffrin, D. J.; Nichols, R. J.; Kuznetsov, A. M.; Zhang, J.; Chi Q.; Ulstrup, J. Single-molecule conductance of redox molecules in electrochemical scanning tunneling microscopy, *J. Phys. Chem. B* **2007**, *111*, 6703-6712.

(52) Albrecht, T.; Moth-Poulsen, K.; Christensen, J. B.; Hjelm, J.; Bjørnholm, T.; Ulstrup, J, Scanning tunneling spectroscopy in an ionic liquid, *J. Am. Chem. Soc.* **2006**, *128*, 6574 – 6575.

(53) Zhou, X. S.; Liu, L.; Fortgang, P.; Lefevre, A. S.; Serra-Muns, A.; Raouafi, N.; Amatore, C.; Mao, B. W.; Maisonhaute, E.; Schollhorn, B., Do Molecular Conductances Correlate with Electrochemical Rate Constants? Experimental Insights. *J. Am. Chem. Soc.* **2011**, *133*, 7509-7516.

(54) Lachmanová, Š. N.; Šebera, J.; Kolivoška, V.; Gasior, J.; Mészáros, G.; Dupeyre, G.; Lainé, P. P.; Hromadová, M. Correlation of electrochemical properties of expanded pyridinium compounds with their single molecule conductance. *Electrochimica Acta*, **2018**, *264*, 301-311.

(55) Lambert, C. Basic concepts of quantum interference and electron transport in single-molecule electronics. *Chem. Soc. Rev.* **2015**, *44*, 875-888.

(56) Sališová, M.; Toma, Š. Acylations of metallocenes with ω-oxo-ω-phenylalkanoyl chlorides. Chlorides of oxo acids as acylating agents. *Chem. Papers* **1986**, *40*, 619-629.

(57) Tombul, M.; Gemici, S.; Bulut, A. Alkyl Lewis Acid Catalyzed Syntheses of Dicarbonyl Ferrocenes. *Asian J. Chem.* **2010**, *22*, 7070-7074.

(58) Xie, R-J.; Han, L-M.; Zhu, N.; Hong, H-L.; Suo, Q-L. The effect of acetyl on the electronic communication of carbon-bridged diferrocene. *J. Coord. Chem.* **2011**, *64*, 3180-3188.

(59) Silva, M. E. N. P. R. A.; Pombiero, A. J. L.; Frausto da Silva, J. J. R.; Herrmann, R.; Deus, N; Bozak, R. E. Redox potential and substituent effects in ferrocene derivatives: II. *J. Organomet. Chem.* **1994**, *480*, 81-90.

(60) Shah, H. H.; Al-Balushi, R. A.; Al-Suti, M. K.; Khan, M. S.; Woodall, C. H.; Molloy, K. C.; Raithby, P. R.; Robinson, T. P.; Dale, S. E. C.; Marken F. Long-Range Intramolecular Electronic Communication in Bis(ferrocenylethynyl) Complexes Incorporating Conjugated Heterocyclic Spacers: Synthesis, Crystallography, and Electrochemistry. *Inorg. Chem.* **2013**, *52*, 4898–4908.

(61) Barlow, S.; O'Hare, D. Metal-Metal Interactions in Linked Metallocenes. *Chem. Rev.* **1997**, *97*, 637-669.

(62) Amatore, C.; Maisonhaute, E.; Schöllhorn, B.; Wadhawan, J. Ultrafast Voltammetry for Probing Interfacial Electron Transfer in Molecular Wires. *ChemPhysChem* **2007**, *8*, 1321–1329.

(63) Savéant, J-M. Effect of Ion Pairing on the Mechanism and Rate of Electron Transfer. Electrochemical Aspects. J. Phys. Chem. B 2001, 105, 8995-9001.

(64) Millone, M.A.D; Hamoudi, H.; Rodríguez, L.; Rubert, A.; Benítez, G.A.; Vela, M.E.; Salvarezza, R.C.; Gayone, J.E.; Sánchez, E.A.; Grizzi, O.; Dablemont, C.; Esaulov, V.A. Self-Assembly of Alkanedithiols on Au(111) from Solution: Effect of Chain Length and Self-Assembly Conditions. *Langmuir*, **2009**, *25* (22), 12945–12953.

(65) Cortés, E.; Rubert, A.A.; Benitez, G.; Carro, P.; Vela, M.E.; Salvarezza, R.C. Enhanced Stability of Thiolate Self-Assembled Monolayers (SAMs) on Nanostructured Gold Substrates. *Langmuir*, **2009**, *25* (10), 5661–5666.

(66) Vericat, C.; Vela, M.E.; Andreasen, G.; Salvarezza, R.C.; Vázquez, L.; Martín-Gago, J.A. Sulfur−Substrate Interactions in Spontaneously Formed Sulfur Adlayers on Au(111). *Langmuir*, **2001**, *17* (16), 4919–4924.

(67) Fischer, J.A.; Zoldan, V.C.; Benitez, G.; Rubert, A.A.; Ramirez, E.A.; Carro, P.; Salvarezza, R.C.; Pasa, A.A.; Vela, M.E. Sulfidization of Au(111) from Thioacetic Acid: An Experimental and Theoretical Study. *Langmuir*, **2012**, 28, 15278–15285.

(68) Lobo Maza, F.; Méndez De Leo, L.; Rubert, A.A.; Carro, P.; Salvarezza, R.C.; Vericat, C. New Insight into the Interface Chemistry and Stability of Glutathione Self-Assembled Monolayers on Au(111). *J. Phys. Chem. C*, **2016**, 120, 14597–14607.

(69) Ramírez, E.A.; Cortés, E.; Rubert, AA.; Carro, P.; Benítez, G.; Vela, M.E.; Salvarezza R.C. Complex Surface Chemistry of 4-Mercaptopyridine Self-Assembled Monolayers on Au(111). *Langmuir*, **2012**, *28* (17), 6839–6847.

(70) Azcárate, J.C.; Addato, M.A.F.; Rubert, A.; Corthey, G.; Moreno, G.S.K.; Benítez, G.; Zelaya, E.; Salvarezza, R.C.; Fonticelli, M.H. Surface Chemistry of Thiomalic Acid Adsorption on Planar Gold and Gold Nanoparticles. *Langmuir*, **2014**, *30* (7), 1820–1826.

(71) Yan, J.; Ouyang, R.; Jensen, P.S.; Ascic, E.; Tanner,D.; Mao, B.; Zhang, J.; Tang,C.; Hush, N.S.; Ulstrup, J.; Reimers J.R. Controlling the Stereochemistry and Regularity of Butanethiol Self-Assembled Monolayers on Au(111). *J. Am. Chem. Soc.* **2014**, *136*, 17087−17094.